Direct knock-on of desolvated ions governs strict ion selectivity in K+ channels

Kopec, Wojciech ; Köpfer, David A. ; Vickery, Owen N.; Bondarenko, Anna S. ; Jansen, Thomas L.C. ; De Groot, Bert L.

Published in:
Nature Chemistry

DOI:
10.1038/s41557-018-0105-9

Publication date:
2018

Document Version
Peer reviewed version

Direct knock-on of desolvated ions governs strict ion selectivity in K^+ channels

Wojciech Kopec[1], David A. Köpfer[1], Owen N. Vickery[2,3], Anna S. Bondarenko[4], Thomas L.C. Jansen[4], Bert L. de Groot[1*], Ulrich Zachariae[2,3*]

[1]Biomolecular Dynamics Group, Max Planck Institute for Biophysical Chemistry, 37077 Göttingen, Germany.

[2]Computational Biology, School of Life Sciences, University of Dundee, Dundee DD1 5EH, United Kingdom.

[3]Physics, School of Science and Engineering, University of Dundee, Dundee DD1 4NH, United Kingdom.

[4]University of Groningen, Zernike Institute for Advanced Materials, 9747 AG Groningen, The Netherlands.

*Corresponding author. E-mail: bgroot@gwdg.de (B.L.d.G.), u.zachariae@dundee.ac.uk (U.Z.)

ABSTRACT

The seeming contradiction that K^+ channels conduct K^+ ions at maximal throughput rates while not permeating the slightly smaller Na^+ ion has perplexed scientists for decades. Although numerous models have addressed selective permeation in K^+ channels, the combination of conduction efficiency and ion selectivity has not yet been linked through a unified functional model. Here, we investigate the mechanism of ion selectivity through atomistic simulations totalling more than 400 microseconds in length, which include over 7000 permeation events. Together with free-energy calculations, our simulations show that both rapid permeation of K^+ and ion selectivity are ultimately based on a single principle: the direct knock-on of completely desolvated ions in the channels' selectivity filter. Herein, the strong interactions between multiple 'naked' ions in the four filter binding sites give rise to a natural exclusion of any competing ions. Our results are in excellent agreement with experimental selectivity data, measured ion interaction energies, and recent two-dimensional infrared spectra of filter ion configurations.

Ionic currents through K^+ channels establish the membrane voltage in all cells and terminate action potentials in electrically excitable cells. K^+ channels facilitate the passage of K^+ ions to near-diffusion limited rates, while reliably excluding smaller Na^+ ions[1,2]. How K^+ channels achieve the combination of these seemingly incompatible features has intrigued scientists for decades[3-7]. A clear separation between K^+ and Na^+ currents is necessary to ensure sharp action potentials, facilitating the rapid propagation of electric signals in excitable cells such as neurons. However, despite intense efforts, a unified explanation for how K^+ channels maintain strict K^+ selectivity under maximal ion conduction rates has remained elusive.

Ions pass through the K^+ channels' selectivity filter (SF), which represents their conserved functional core, enabling rapid and selective ion permeation[8]. It contains four successive K^+ binding sites (S_1-S_4), with two additional binding sites at its extracellular entrance (S_0) and in the water-filled central cavity (S_{cav})[9] (Fig. 1A). Predating structural elucidation of the channels, the snug-fit model, still preferred by most present textbooks[10,11], posited that the K^+ binding sites in a rigid SF provide an unfavourable binding environment for the smaller Na^+ ions[4]. Upon determination of the first K^+ channel structures by x-ray crystallography, the electron density observed in the SF K^+ binding sites was interpreted to reflect alternate occupation with water and ions[1,12,13]. This conclusion informed subsequent structure-based and computational models[14-22], which suggested that ion selectivity arises from the intrinsic flexibility of specific SF binding sites[14,15], the collective dynamics of ions and water within the SF[16,17], or energetic differences in ion binding[13,14,16-20]. These models were based on the assumption that permeating K^+ ions in the SF are separated by water molecules ('soft knock-on' mechanism). The majority of previous computational studies identified the SF K^+ binding sites as thermodynamically K^+ selective, due to the optimal coordination of a K^+ ion by eight carbonyl ligands, while Na^+ binding of to the same geometry was found to be energetically less favourable[14,18-20,23-25]. However, the complete sequence of microscopic events leading to efficient K^+ permeation and simultaneous Na^+ exclusion during ion permeation has never been revealed, partially due to the inability to observe high, sustained currents in previous atomistic molecular dynamics (MD) simulations[26].

Recently however, a reanalysis of the crystallographic data showed that K^+ ions form close ion pairs (i.e. direct ion-ion contacts) at neighbouring SF ion binding sites[27].

Furthermore, accompanying molecular dynamics simulations suggested that the strong electrostatic interaction between ions at short distance plays a key role in establishing the observed high rates of K^+ ion conduction, while water molecules are largely excluded from permeating the channel[27]. Since the instantaneous ion occupancies of the SF under 'direct Coulomb knock-on' conditions drastically differ from those of 'soft knock-on'[28], the competition between K^+ and Na^+ ions, and therefore the mechanism of ion selectivity, is likely to be based on different principles than previously thought. As it is now possible to directly simulate ion currents and analyse thousands of individual ion permeation events at the atomistic level, we set out to apply this methodology to achieve unfiltered insight into the determinants of ion selectivity in K^+ channels under actual permeation conditions. Our extended simulations spanning more than 400 μs of simulated time allowed us to analyse in detail over 7000 individual ion permeation events.

Our results present a novel mechanism of ion selectivity in K^+ channels providing a unifying explanation for the two major, seemingly irreconcilable, physiological characteristics of K^+ channel conduction – highly efficient ion transfer under exquisite K^+ selectivity. We show that full desolvation of ions in the SF – required to establish close contacts between K^+ ions in the neighbouring sites and rapid conduction – efficiently excludes Na^+ ions from permeating the channel. Importantly, in contrast to previous ion permeation models[29-31], our findings show that any significant level of water co-permeation invariably leads to drastically diminished ion selectivity and reduced ion conduction rates. Finally, we demonstrate that recent K^+ channel data from two-dimensional infrared (2D IR) spectroscopy[30], which were originally interpreted to be exclusively compatible with filter occupancies under water co-permeating conditions, are equally compatible with states displaying directly contacting ions in the SF.

RESULTS

The direct Coulomb knock-on is intrinsically ion-selective

We conducted atomistic simulations to directly investigate the origins of ion selectivity and the coupling of ion and water flux under K^+ channel permeation conditions, employing both electrochemical ion gradients and applied electric fields to generate membrane voltages in the range of 220–300 mV. These acted as driving forces for the permeation of K^+ and Na^+ ions across a variety of channels including KcsA, MthK, Kv1.2, NaK2K and NaK2CNG-N. The data we collected comprise more than 7000 ion permeation events in mixed and pure K^+ and Na^+ solutions (Supplementary Tables 1-9).

We first focused on the most studied K^+ channel KcsA (Fig. 1A). The channel current in KcsA is strongly dominated by permeating K^+ ions in all K^+-containing solutions (Fig. 1B). In mixed solutions of a 2:1 (K^+/Na^+) ratio, the KcsA current shows a K^+/Na^+ permeability ratio of 55:1. Even under excess of Na^+ (1:2 K^+/Na^+ mixture), KcsA favours K^+ permeation with a permeability quotient of 22:1. Only in the complete absence of K^+, a residual Na^+ current of ~15% of the maximum K^+ flux is observed.

K^+ ions permeate the channel in a fully dehydrated state, consistent with the 'direct Coulomb knock-on' mechanism. In pure K^+ solution, we therefore do not observe any co-permeation of water (Fig. 1B). By contrast, Na^+ ions co-permeate with water. As a consequence, few water molecules are carried along during the rare event of Na^+ traversing the SF (Fig. 1C). In both the 2:1 and 1:2 (K^+/Na^+) mixed solutions, the resulting overall water-to-ion flux ratio is about 0.03 ± 0.02 (Fig. 1B). In pure Na^+ solution, the raised Na^+ current leads to increased water permeation, with a water-ion flux ratio of 0.22 ± 0.08.

Experimental studies have reported K^+ channel Na^+/K^+ permeability ratios between 0.006–0.04[5,6,32]. The simulated Na^+/K^+ ratios of 0.02–0.04 are thus in good agreement with available experimental data. Further, for KcsA, we find a reduction in outward K^+ ion current to about one-third of that in pure KCl for the 2:1 (K^+/Na^+) concentration regime, while it decreases to about 20% under Na^+ excess (1:2 mixture; Fig. 1B). This observation reflects the experimental observation of K^+ channel block by intracellular Na^+, which has been widely reported in single-channel

electrophysiology studies[33,34] and is clearly visible in the ionic traces through the SF (Fig. 1C).

The SF of many K^+ channels, including KcsA, undergoes a conformational change at K^+ concentrations below ~20 mM on timescales of up to seconds, preventing ion flux under low-K^+ conditions[1,35,36]. This filter gating or collapse provides an additional layer of ion selectivity to K^+ channels. On the shorter timescale of our simulations, however, the SF remains in the conductive state. Our observations made in pure Na^+ solutions are therefore compared to experiments on the constitutively conductive SF variant, $KcsA^{D\text{-}Ala77}$, in which filter collapse is sterically blocked. In experiments, this semisynthetic channel form conducts Na^+ when K^+ is completely absent, with currents similar to those we observe, while as in our simulations, the addition of K^+ disrupts Na^+ conduction[35]. The experimentally recorded ratio between maximum K^+ and residual Na^+ current in $KcsA^{D\text{-}Ala77}$ is in remarkably good agreement with our findings[35].

Strict K^+ selectivity is coupled to the exclusion of water

Next, we expanded our investigation to the bacterial MthK and the eukaryotic Kv1.2 channel (W362Y variant) as well as the engineered channels NaK2CNG-N and NaK2K (Fig. 2A). NaK2K and NaK2CNG-N are both generated by introducing mutations in the SF of the non-selective bacterial ion channel NaK[37,38]. The SF of NaK possesses only two ion binding sites, which are chemically equivalent to sites S3 and S4 of canonical K^+ channels, and displays bound water molecules within a widened vestibule[39,40]. In NaK2CNG-N, the NaK SF is modified to yield three consecutive ion binding sites (S2-S4), while in NaK2K, the mutations reconstruct a canonical K^+ channel SF with four consecutive ion binding sites[38]. In experiments, MthK, Kv1.2 and NaK2K are strongly K^+ selective, while NaK2CNG-N shows similar permeability for both K^+ and Na^+ [41,42].

The diminished K^+ selectivity of the NaK and NaK2CNG channels has previously been associated with the reduced number of SF ion binding sites[38], the increased hydration level of ions[22,43,44], for instance seen in the NaK crystal structure[39,40], and enhanced structural plasticity of the SF[45]. This led to the conclusion that only channels with four consecutive ion binding sites in the SF can ensure fully K^+

selective ion permeation. However, the mechanistic basis for this phenomenon has remained unclear, in particular under permeation conditions[38,42,46].

In our simulations, we find strictly K^+ selective current in KcsA, MthK, NaK2K, and Kv1.2 W362Y (Fig. 2B). The total channel current shows some differences for pure K^+ solution. In mixed K^+/Na^+ solutions, the current overwhelmingly arises from K^+ permeation events, both under excess of K^+ and Na^+. In pure Na^+, only KcsA and NaK2K give rise to appreciable Na^+ fluxes.

By contrast, NaK2CNG-N shows a greatly reduced K^+ selectivity with considerable Na^+ permeation in the K^+/Na^+ mixtures, as well as the largest level of Na^+ current in pure Na^+ amongst all of the investigated channels. It also displays the lowest K^+ current in pure K^+ solution. Notably, the Na^+ current is linked to a substantially raised level of water co-permeation. While the water-to-ion flux ratio is very small in all of the strictly K^+ selective channels (below 0.05 in all regimes in which K^+ is present), the absence of the fourth binding site in NaK2CNG-N leads to a much diminished exclusion of water, both during Na^+ and K^+ permeation, and thus allows both ion types to traverse the SF with similar probability. We observe a water-ion ratio of >>1 under all ionic regimes in NaK2CNG-N, showing that a significant part of the ions' solvation shell is retained in the SF during permeation. These observations are in accordance with previous experiments, in which mutations reducing the number of K^+ binding sites in the SF from four to three abolished K^+ selectivity[38,42], and explain these experimental observations by insufficient exclusion of hydrating water around the ions. Structurally, we find that increased co-permeation of water is underpinned by an enhanced flexibility of the NaK2CNG-N SF with regard to filters with four ion binding sites. These dynamics cause a small widening of the SF on average, and thereby slightly relax the strict geometric constraints for ion transfer, especially at the central ion binding site. Similar findings have recently been reported for the related NaK channel[45].

Fully desolvated ions in the SF are in agreement with 2D-IR spectroscopy experiments

All of these observations suggested that the strict exclusion of water, and ion conduction by the direct Coulomb knock-on mechanism, underpin ion selectivity in K^+ channels under permeation conditions. We therefore re-examined a recent

investigation, in which equilibrium molecular dynamics simulations were used to interpret 2D-IR spectra on the isotope-labeled SF of synthetic KcsA under no voltage. In this study, it was found that only IR spectra that were predicted from simulations of water-and-ion occupied SFs were compatible with the experimental data, after fitting the relative population of each state and additionally taking carbonyl-flipped SF conformations into consideration[30].

By contrast, SF ion populations under non-equilibrium ion flux conditions were not fitted to match the IR data, but rather taken directly from our previous simulations which were conducted under voltage[27]. As shown in the present work, these K^+ conducting states display direct ion-ion contacts. The corresponding spectra of these conducting states were interpreted to disagree with the IR experiments, which led to the conclusion that water molecules are required to accompany K^+ ions during ion permeation.

To reconcile this apparent discrepancy, we used our previously reported ion configurations (together with those shown here) in the ion-conductive SF, and equilibrated these states further at 0 mV to replicate the conditions of the IR experiment (see Supplementary Methods and Supplementary Table 10). We then followed the same protocol employed in previous studies[30] to calculate the final IR spectra. Spectra calculated from a weighted (fitted) combination of these states yield good agreement with the experimental spectra, similar to a weighted sum of the water-containing states described previously and independently repeated by us (the final spectra are shown in Fig. 3 and Supplementary Fig. 4). Furthermore, when configurations with only direct ion-ion contacts in the SF are taken into consideration, a wide range of spectral parameters such as peak positions, nodal slopes and intensity ratios, are also consistent with the experimental data (Table 1). We conclude that the analysis based on 2D-IR spectra cannot differentiate between the two scenarios of SF occupancy and thus could support both mechanisms of ion permeation with and without co-permeating water.

How does ion dehydration contribute to selectivity?

The number of K^+ and Na^+ ions traversing KcsA from the intracellular side during conduction shows a strong divergence upon SF entry (Supplementary Fig. 6). The fraction of Na^+ ions migrating from S_4 to S_3 decreases by about 18-fold, while that of K^+ remains nearly constant. Overall, in pure KCl, 44% of all K^+ ions entering the SF at S_4 eventually permeate fully, compared to only 2.5% of Na^+ ions in pure NaCl (the presence of K^+ reduces this proportion further to less than 1%; Supplementary Fig. 7).

Since Na^+ interacts more strongly with water than K^+, the free energy required to fully dehydrate Na^+ ions exceeds that of K^+ by 74.8 kJ/mol (see Supplementary Methods and Supplementary Fig. 8). This energy difference contributes to the thermodynamic basis for ion selectivity at every SF site. Free energy calculations on occupancy states with direct ion-ion contacts, i.e. states that lead to high-efficiency ion permeation under voltage (Supplementary Fig. 8), show that all of the internal SF K^+ binding sites in KcsA are K^+ selective when this dehydration free energy is taken into account (Supplementary Fig. 8). In particular, the SF entry sites S_4 and S_1 favour K^+ binding by up to 27.6 kJ/mol. By contrast, sites in-plane with the filter carbonyl groups between the K^+ binding positions remain slightly Na^+-selective, in agreement with our findings from ion flux simulations.

The SF is too narrow to allow ions to permeate in the presence of their full hydration shells. Most ions therefore enter and pass through the SF either in a partially or fully dehydrated state. The vast majority of permeation events we observe follow the 'direct Coulomb knock-on' mechanism, where K^+ ions traverse the SF of selective channels without hydrating water.

In contrast, the classic 'soft knock-on' mechanism, in which one water molecule permeates along with each ion in the SF, would compromise the maximal dehydration of permeating ions. According to our observations, the thermodynamic basis for ion selectivity is thus optimised when the maximum number of solvating water molecules is removed upon entry into the SF. Simultaneously, direct contacts between fully dehydrated ions lead to maximally efficient ion permeation in our simulations. We therefore identify the complete loss of the ion hydration shell during SF entry, induced by the unique architecture of the SF, as the major contributing factor underpinning both ion selectivity and high conduction rates.

Thermodynamic and kinetic factors of selective ion permeation within the SF

Finally, we aimed to resolve the processes that contribute to selectivity when residual Na^+ ions compete with K^+ ions within the SF. To distinguish thermodynamic effects (e.g., differential affinity of K^+ and Na^+ to filter binding sites)[25] from kinetic effects, which may inhibit the passage of ion types between the binding sites[7], we recorded K^+ and Na^+ density profiles in the SF, based on KcsA simulation data under various ion concentration regimes (Supplementary Fig. 9). Although these density profiles do not strictly reflect equilibrium free energies, we use them here as an approximate measure to quantify differences in binding affinity for K^+ and Na^+ in the SF (manifested as different density minima) and kinetic barriers (peak heights).

Due to their high K^+ affinity, the SF binding sites S_4–S_0 show strong K^+ density in pure KCl solutions. Lower minima for K^+ compared to Na^+ in mixed K^+/Na^+ conditions demonstrate the channel's thermodynamic K^+ selectivity, which we also observe in free energy calculations (Supplementary Fig. 8). Considering transition kinetics, large barriers occur for Na^+ transfer between S_3–S_2 and near S_1, however they do not exceed the maximum barrier to K^+ translocation between S_4–S_3. Only under excess of Na^+, slightly raised kinetic barriers for Na^+ transfer are observed.

However, in contrast to K^+ ions, the Na^+ density shows additional Na^+ binding sites between the canonical K^+ positions, located in-plane with the backbone carbonyl oxygen atoms. These sites can be observed even in the absence of K^+, but under K^+ excess, Na^+ occupation mainly shifts to positions between the K^+ binding sites S_3–S_4, S_1–S_2 (Supplementary Fig. 9). As a consequence, the distance between two favourable Na^+ binding positions in the SF centre increases to ~7 Å, more than twice the distance observed for a K^+ ion pair at S_2 and S_3, which we have found to be crucial for high-speed conduction of K^+[27].

The simultaneous presence of K^+ and Na^+ in the SF therefore has a major effect on the SF occupancy pattern, as under excess of K^+, binding of Na^+ between the K^+ positions leads to a disruption of the optimal ion-ion distance for efficient conduction. Accordingly, Na^+ ions cannot permeate the channels at high kinetic rates to generate sizable Na^+ currents, and they instead block K^+ conduction, as observed in experiments[33,34] and also suggested by calculations of potentials of mean force in a previous computational study[23].

Since the typical ion concentration of K^+ is 140 mM and that of Na^+ is near 10 mM in the cytoplasm[47], only few Na^+ ions would typically compete with an excess of K^+ ions during their physiological outward permeation. As there is a higher concentration of Na^+ on the extracellular side of the membrane, we also investigated the selectivity for extracellular Na^+ upon outward (and also inward) K^+ flux in additional sets of simulations (Supplementary Figs. 10-11), confirming strict selectivity also under these conditions.

DISCUSSION

The results we present demonstrate an intimate relationship between ion selectivity, rapid ion conduction, and the dehydration of permeating ions in K^+ channels (Fig. 4). They also highlight the additional role of complex multi-ion interactions between the preferred K^+ ions and competing Na^+ ions within the SF for enhanced selectivity.

Across a range of different channel types, we show that the level of water co-permeation in the SF is closely linked to the ion selectivity and conduction efficiency of the channels. An increased amount of water in the SF invariably decreases both, conduction rates and ion selectivity (Fig. 2; Supplementary Figs. 12-14). Channels with only three K^+ binding sites in their SF do not dehydrate permeating ions to the same degree as the canonical K^+ channels, which possess four stacked ion binding positions in their filter. As a consequence, they lack the exquisite ion selectivity of the canonical K^+ channels (Fig. 4). The selectivity for K^+ is optimised when the ions are maximally dehydrated, as observed for example for the KcsA, MthK and NaK2K channels. Notably, Na^+ channels possess a much wider SF (~8 Å) than K^+ channels (~3 Å)[48], and consequently, Na^+ ions permeate these channels in a mostly hydrated form[49].

In all of the K^+ channel types we investigated, Na^+ ions typically cross the SF together with some remaining hydrating water molecules. In the SF of the selective channel types, competing K^+ ions however displace residual Na^+ ions to positions located between the crystallographically determined K^+ binding sites, where they cannot fulfill the criterion for highly efficient ion conduction, i.e. ion pair formation in the K^+ binding sites (Fig. 4, centre). Free energy calculations also identify these intermediate sites as preferred positions for Na^+ binding (Supplementary Fig. 8). These results, together with the data we obtain from analysing ~7000 individual permeation events,

therefore challenge the snug-fit model, which posits that the smaller Na^+ is coordinated less optimally than K^+ by the carbonyl groups of the canonical SF K^+ binding sites. This model is, to date, cited most often as the basis for K^+ channel selectivity in current textbooks[10,11] despite having been disproven many times[14,18,19,23,50]. Our results now combine aspects of the previously proposed alternative mechanisms into a unified model, which simultaneously explains rapid ion permeation and selectivity by multi-ion, direct Coulomb knock-on.

This mechanism is in agreement with a wide array of available experimental data, including crystallographic, electrophysiological and spectroscopic investigations. By calculating 2D IR spectra for a large number of possible occupancy states of the SF, and by using the same averaging scheme as used in previous work[30], we demonstrate that states which exclusively display direct ion-ion contacts in the SF are fully compatible with recent experimental 2D-IR spectra. Notably, the carbonyl-flipped states that are necessary to explain the IR data on the basis of water-separated ion configurations in the SF correspond to non-conductive filter states in our simulations in all K^+ channels except in the non-selective NaK2CNG-N. Moreover, our observations explain the results from previous experiments studying the interactions of a range of cations with K^+ channels (see Supplementary Text in SI)[51]. We therefore obtain a convergent picture of high-conductance K^+ channel permeation and exquisite ion selectivity based on maximally dehydrated ions, which occupy neighbouring positions in a linear array of at least four SF ion binding sites. In this unified model, efficient throughput and strict selectivity are no longer contradictory, but arise as two necessary consequences of a single mechanism.

METHODS

Computational electrophysiology simulations

We studied spontaneous ion permeation through potassium channels, in pure and mixed K^+/Na^+ solutions, driven by the transmembrane voltage induced by charge imbalances as implemented in the CompEL (computational electrophysiology) method in GROMACS[52,53]. For open-state KcsA, we used the x-ray structure (PDB id: 3f5w[54]), with the selectivity filter in the conductive configuration (PDB id: 1k4c[1]), embedded in a patch of a POPC membrane, as reported in our previous simulations[27]. For open-state MthK, we used the high resolution structure of an open state (PDB id: 3ldc (ref)). For open-state Kv1.2 we used the pore domain from the 'paddle-chimera' Kv1.2-Kv2.1 structure (PDB id: 2r9r), that remains open in simulation at positive voltages)[26]. For the open-state NaK2K and NaK2CNG-N, we used high resolution structures (PDB id: 3ouf and 3k06). All simulations were carried out with GROMACS 5.0 or 5.1[55-58], using the dual membrane setup typical of the CompEL scheme, with an ionic imbalance between the compartments of $2e^-$, yielding a transmembrane voltage of ~220mV or by applying an external electric field[59] yielding a transmembrane voltage of ~280 mV. The ionic currents were estimated by counting the number of ions permeating the SF in time. A list of all simulations is shown in Tables S1-S9. All simulation details and simulation description of other channels are provided in the SI. Kv1.2 W362Y was used instead of WT Kv1.2 due to SF instabilities in MD simulations (see Supplementary Fig. 14). An equivalent mutation in Kv1.6 yields a channel with almost the same conduction and selectivity properties as WT Kv1.6[60] (see also SI). In NaK2K and NaK2CNG-N the F92A mutation was used to increase the ionic current, as in experiments[42].

2D IR spectral calculations

In our 2D IR calculations, we used a single KcsA channel embedded in a POPC membrane, similar to the system reported in Kratochvil et al.[30]. We used the SF occupancy states observed in our computational electrophysiology simulations, and compared them with the experimental spectrum. To do so, a number of specific occupancy states of the SF, corresponding to ion-conductive configurations, were selected (see Supplementary Table 3), and further equilibrated at 0 mV for 10 ns per state, to mimic the conditions of the IR experiments. Subsequently, a number of snapshots (at least 9 per single occupancy state) were randomly selected from the last 2 ns of equilibration. Each snapshot was then used as a starting point for a simulation of 1 ns length, during which the positions of atoms were saved every 20 fs. These trajectories were then used for spectral calculations. The spectral calculations were performed by first extracting the amide I Hamiltonian, transition dipoles and site frequencies from the 1 ns trajectories. Next, the amide units corresponding to those labeled in the experiment[30], were selected and their frequencies were shifted by -66 cm^{-1} to account for the isotope label. 1D and 2D IR spectra were calculated with the numerical integration of the Schrödinger equation method (NISE)[61,62]. The linear 1D spectrum is then obtained by a Fourier transform of the linear response function, while the 2D spectrum is obtained with a two-dimensional Fourier transform with respect to the coherence times. Full computational procedure is described in the SI.

Free energy calculations

We performed free energy calculations for individual binding sites in the SF of KcsA to assess their thermodynamic selectivity between K^+ and Na^+ ions, for the occupancy

states most frequently visited during ion permeation. Consequently, we focused on KK0K and 0KKK occupancies (Supplementary Figure 8). Three snapshots per occupancy pattern were selected from the computational electrophysiology simulations, transformed back to a single membrane setup, and further equilibrated for 40 ns at 0 mV. The final snapshots from these simulations were then used for K^+ to Na^+ alchemical free energy calculations to obtain $\Delta G_{K,Na}^{site}$ for each occupied site. To assess the existence and selectivity of potential Na^+ binding sites in the SF, as previously suggested[13,25], we introduced a single Na^+ ion instead of a K^+ ion at each site for both starting occupancies, ultimately resulting in the following occupancies: KNaK, NaKK, KKNa (Fig. 3B). After 40 ns of equilibration, the introduced Na^+ ions bound to their preferred binding sites, in plane with four SF carbonyl oxygen atoms. The final snapshots from these simulations were then used for Na^+ to K^+ alchemical free energy calculations. To calculate the free energy differences between K^+ and Na^+, we employed the free energy code in GROMACS. The free energy differences were calculated using the Multistate Bennett Acceptance Ratio (MBAR) method[63] as implemented in the 'alchemical analysis' utility[64]. The full computational procedure is described in the SI.

REFERENCES

1 Zhou, Y., Morais-Cabral, J. H., Kaufman, A. & MacKinnon, R. Chemistry of ion coordination and hydration revealed by a K+ channel-Fab complex at 2.0 A resolution. *Nature* **414**, 43-48 (2001).

2 MacKinnon, R. Potassium channels and the atomic basis of selective ion conduction (Nobel Lecture). *Angew. Chem. Int. Ed.* **43**, 4265-4277 (2004).

3 Mullins, L. J. An analysis of conductance changes in squid axon. *J. Gen. Physiol.* **42**, 1013-1035 (1959).

4 Bezanilla, F. & Armstrong, C. M. Negative conductance caused by entry of sodium and cesium ions into the potassium channels of squid axons. *J. Gen. Physiol.* **60**, 588-608 (1972).

5 Hille, B. Potassium channels in myelinated nerve. Selective permeability to small cations. *J. Gen. Physiol.* **61**, 669-686 (1973).

6 Neyton, J. & Miller, C. Discrete Ba2+ block as a probe of ion occupancy and pore structure in the high-conductance Ca2+ -activated K+ channel. *J. Gen. Physiol.* **92**, 569-586 (1988).

7 Nimigean, C. M. & Allen, T. W. Origins of ion selectivity in potassium channels from the perspective of channel block. *J. Gen. Physiol.* **137**, 405-413 (2011).

8 MacKinnon, R., Cohen, S. L., Kuo, A., Lee, A. & Chait, B. T. Structural conservation in prokaryotic and eukaryotic potassium channels. *Science* **280**, 106-109 (1998).

9 Doyle, D. A. *et al.* The structure of the potassium channel: molecular basis of K+ conduction and selectivity. *Science* **280**, 69-77 (1998).

10 Alberts, B. *et al. Molecular Biology of the Cell. 4th edition*. (Garland Science, 2002).

11 Steven, A., Baumeister, W., Johnson, L. N. & Perham, R. N. *Molecular Biology of Assemblies and Machines*. (Garland Science, 2016).

12 Zhou, Y. & MacKinnon, R. The occupancy of ions in the K+ selectivity filter: charge balance and coupling of ion binding to a protein conformational change underlie high conduction rates. *J. Mol. Biol.* **333**, 965-975 (2003).

13 Thompson, A. N. *et al.* Mechanism of potassium-channel selectivity revealed by Na(+) and Li(+) binding sites within the KcsA pore. *Nat. Struct. Mol. Biol.* **16**, 1317-1324 (2009).

14 Noskov, S. Y., Berneche, S. & Roux, B. Control of ion selectivity in potassium channels by electrostatic and dynamic properties of carbonyl ligands. *Nature* **431**, 830-834 (2004).

15 Noskov, S. Y. & Roux, B. Ion selectivity in potassium channels. *Biophys. Chem.* **124**, 279-291 (2006).

16 Aqvist, J. & Luzhkov, V. Ion permeation mechanism of the potassium channel. *Nature* **404**, 881-884 (2000).

17 Medovoy, D., Perozo, E. & Roux, B. Multi-ion free energy landscapes underscore the microscopic mechanism of ion selectivity in the KcsA channel. *Biochim. Biophys. Acta* **1858**, 1722-1732 (2016).

18 Bostick, D. L. & Brooks, C. L., 3rd. Selectivity in K+ channels is due to topological control of the permeant ion's coordinated state. *Proc. Natl. Acad. Sci. U.S.A* **104**, 9260-9265 (2007).

19 Thomas, M., Jayatilaka, D. & Corry, B. The predominant role of coordination number in potassium channel selectivity. *Biophys. J.* **93**, 2635-2643 (2007).

20 Varma, S. & Rempe, S. B. Tuning ion coordination architectures to enable selective partitioning. *Biophys. J.* **93**, 1093-1099 (2007).
21 Shrivastava, I. H., Tieleman, D. P., Biggin, P. C. & Sansom, M. S. K(+) versus Na(+) ions in a K channel selectivity filter: a simulation study. *Biophys. J.* **83**, 633-645 (2002).
22 Fowler, P. W., Tai, K. & Sansom, M. S. The selectivity of K+ ion channels: testing the hypotheses. *Biophys. J.* **95**, 5062-5072 (2008).
23 Furini, S. & Domene, C. Selectivity and permeation of alkali metal ions in K+-channels. *J. Mol. Biol.* **409**, 867-878 (2011).
24 Egwolf, B. & Roux, B. Ion selectivity of the KcsA channel: a perspective from multi-ion free energy landscapes. *J. Mol. Biol.* **401**, 831-842 (2010).
25 Kim, I. & Allen, T. W. On the selective ion binding hypothesis for potassium channels. *Proc. Natl. Acad. Sci. U.S.A* **108**, 17963-17968 (2011).
26 Jensen, M. O., Jogini, V., Eastwood, M. P. & Shaw, D. E. Atomic-level simulation of current-voltage relationships in single-file ion channels. *J. Gen. Physiol.* **141**, 619-632 (2013).
27 Kopfer, D. A. *et al.* Ion permeation in K(+) channels occurs by direct Coulomb knock-on. *Science* **346**, 352-355 (2014).
28 Furini, S. & Domene, C. Atypical mechanism of conduction in potassium channels. *Proc. Natl. Acad. Sci. U.S.A* **106**, 16074-16077 (2009).
29 Berneche, S. & Roux, B. Energetics of ion conduction through the K+ channel. *Nature* **414**, 73-77 (2001).
30 Kratochvil, H. T. *et al.* Instantaneous ion configurations in the K+ ion channel selectivity filter revealed by 2D IR spectroscopy. *Science* **353**, 1040-1044 (2016).
31 Heer, F. T., Posson, D. J., Wojtas-Niziurski, W., Nimigean, C. M. & Berneche, S. Mechanism of activation at the selectivity filter of the KcsA K(+) channel. *Elife* **6** (2017).
32 LeMasurier, M., Heginbotham, L. & Miller, C. KcsA: it's a potassium channel. *J. Gen. Physiol.* **118**, 303-314 (2001).
33 Heginbotham, L., LeMasurier, M., Kolmakova-Partensky, L. & Miller, C. Single streptomyces lividans K(+) channels: functional asymmetries and sidedness of proton activation. *J. Gen. Physiol.* **114**, 551-560 (1999).
34 Nimigean, C. M. & Miller, C. Na+ block and permeation in a K+ channel of known structure. *J. Gen. Physiol.* **120**, 323-335 (2002).
35 Valiyaveetil, F. I., Leonetti, M., Muir, T. W. & Mackinnon, R. Ion selectivity in a semisynthetic K+ channel locked in the conductive conformation. *Science* **314**, 1004-1007 (2006).
36 Domene, C. & Furini, S. Dynamics, energetics, and selectivity of the low-K+ KcsA channel structure. *J. Mol. Biol.* **389**, 637-645 (2009).
37 Shi, N., Ye, S., Alam, A., Chen, L. & Jiang, Y. Atomic structure of a Na+- and K+-conducting channel. *Nature* **440**, 570-574 (2006).
38 Derebe, M. G. *et al.* Tuning the ion selectivity of tetrameric cation channels by changing the number of ion binding sites. *Proc. Natl. Acad. Sci. U.S.A* **108**, 598-602 (2011).
39 Alam, A. & Jiang, Y. High-resolution structure of the open NaK channel. *Nat. Struct. Mol. Biol.* **16**, 30-34 (2009).
40 Alam, A. & Jiang, Y. Structural analysis of ion selectivity in the NaK channel. *Nat. Struct. Mol. Biol.* **16**, 35-41 (2009).

41 Derebe, M. G., Zeng, W., Li, Y., Alam, A. & Jiang, Y. Structural studies of ion permeation and Ca2+ blockage of a bacterial channel mimicking the cyclic nucleotide-gated channel pore. *Proc. Natl. Acad. Sci. U.S.A* **108**, 592-597 (2011).
42 Sauer, D. B., Zeng, W., Canty, J., Lam, Y. & Jiang, Y. Sodium and potassium competition in potassium-selective and non-selective channels. *Nat. Commun.* **4**, 2721 (2013).
43 Thomas, M., Jayatilaka, D. & Corry, B. Mapping the importance of four factors in creating monovalent ion selectivity in biological molecules. *Biophys. J.* **100**, 60-69 (2011).
44 Noskov, S. Y. & Roux, B. Importance of hydration and dynamics on the selectivity of the KcsA and NaK channels. *J. Gen. Physiol.* **129**, 135-143 (2007).
45 Shi, C. *et al.* A single NaK channel conformation is not enough for non-selective ion conduction. *Nat. Commun.* **9**, 717 (2018).
46 Furini, S. & Domene, C. Nonselective conduction in a mutated NaK channel with three cation-binding sites. *Biophys. J.* **103**, 2106-2114 (2012).
47 Lodish, H. *et al. Molecular Cell Biology. 5th edition*. (W. H. Freeman, 2003).
48 Zhekova, H. R., Ngo, V., da Silva, M. C., Salahub, D. & Noskov, S. Selective ion binding and transport by membrane proteins – A computational perspective. *Coord. Chem. Rev.* **345**, 108-136 (2017).
49 Payandeh, J., Scheuer, T., Zheng, N. & Catterall, W. A. The crystal structure of a voltage-gated sodium channel. *Nature* **475**, 353-358 (2011).
50 Roux, B. *et al.* Ion selectivity in channels and transporters. *J. Gen. Physiol.* **137**, 415-426 (2011).
51 Lockless, S. W. Structural and Thermodynamic Properties of Selective Ion Binding in a K(+) Channel. *PLoS Biol.* **5** (2007).
52 Kutzner, C., Grubmuller, H., de Groot, B. L. & Zachariae, U. Computational electrophysiology: the molecular dynamics of ion channel permeation and selectivity in atomistic detail. *Biophys. J.* **101**, 809-817 (2011).
53 Kutzner, C. *et al.* Insights into the function of ion channels by computational electrophysiology simulations. *Biochim. Biophys. Acta* **1858**, 1741-1752 (2016).
54 Cuello, L. G., Jogini, V., Cortes, D. M. & Perozo, E. Structural mechanism of C-type inactivation in K(+) channels. *Nature* **466**, 203-208 (2010).
55 Van Der Spoel, D. *et al.* GROMACS: fast, flexible, and free. *J. Comput. Chem.* **26**, 1701-1718 (2005).
56 Hess, B., Kutzner, C., van der Spoel, D. & Lindahl, E. GROMACS 4: Algorithms for Highly Efficient, Load-Balanced, and Scalable Molecular Simulation. *J. Chem. Theory Comput.* **4**, 435-447 (2008).
57 Pronk, S. *et al.* GROMACS 4.5: a high-throughput and highly parallel open source molecular simulation toolkit. *Bioinformatics* **29**, 845-854 (2013).
58 Abraham, M. J. *et al.* GROMACS: High performance molecular simulations through multi-level parallelism from laptops to supercomputers. *SoftwareX* **1–2**, 19-25 (2015).
59 Roux, B. The membrane potential and its representation by a constant electric field in computer simulations. *Biophys. J.* **95**, 4205-4216 (2008).
60 Sauer, D. B., Zeng, W., Raghunathan, S. & Jiang, Y. Protein interactions central to stabilizing the K+ channel selectivity filter in a four-sited

configuration for selective K+ permeation. *Proc. Natl. Acad. Sci. U.S.A* **108**, 16634-16639 (2011).
61 Jansen, T. & Knoester, J. Nonadiabatic effects in the two-dimensional infrared spectra of peptides: application to alanine dipeptide. *J. Phys. Chem. B* **110**, 22910-22916 (2006).
62 Liang, C. & Jansen, T. L. An Efficient N(3)-Scaling Propagation Scheme for Simulating Two-Dimensional Infrared and Visible Spectra. *J. Chem. Theory Comput.* **8**, 1706-1713 (2012).
63 Shirts, M. R. & Chodera, J. D. Statistically optimal analysis of samples from multiple equilibrium states. *J. Chem. Phys.* **129**, 124105 (2008).
64 Klimovich, P. V., Shirts, M. R. & Mobley, D. L. Guidelines for the analysis of free energy calculations. *J. Comput. Aided Mol. Des.* **29**, 397-411 (2015).

ACKNOWLEDGEMENTS

We thank Helmut Grubmüller, Simon Bernèche, Florian Heer and Salomé Llabrés for helpful discussions. Supported by the German Research Foundation DFG through FOR 2518 'DynIon', Project P5 (W.K. and B.L.d.G), the Scottish Universities' Physics Alliance (U.Z.) and the BBSRC (training grant BB/J013072/1, O.N.V. and U.Z.). All data and analysis scripts are archived at the Max Planck Institute for Biophysical Chemistry archives and available upon request.

AUTHOR CONTRIBUTIONS

U.Z. and B.L.d.G. conceived and supervised the project. W.K. performed and analysed ion channel simulations under ion gradients and voltage, free energy simulations, and IR spectral calculations. D.A.K performed and analysed KcsA and initial MthK simulations. O.N.V. performed and analysed additional ion channel simulations under voltage. A.S.B. assisted with IR spectral calculations. T.L.C.J. designed and supervised spectral IR calculations. W.K., D.A.K., O.N.V. and U.Z. prepared the figures, and U.Z., B.L.d.G. and W.K. wrote the manuscript with comments from all authors.

COMPETING INTEREST STATEMENT

The authors declare no competing interests.

DATA AVAILABILITY

All relevant data are available from the authors upon request.

AVAILABILITY OF COMPUTER CODE

Custom computer code used for simulation analysis is available from the authors upon request.

FIGURE CAPTIONS

Fig. 1: Ion selectivity of KcsA. (a) Open state form of KcsA with the main K^+ binding sites of the SF (S_1–S_4) at the interface between the four channel subunits. **(b)** KcsA currents and water/ion permeation ratios at a voltage of ~220 mV in solutions of 300 mM ionic strength containing both K^+ and Na^+ ions. At a 2:1 excess of K^+, less than 2% of the current originates from Na^+ flux (K^+: purple; Na^+: yellow), corresponding to a selectivity of 55:1 for K^+ over Na^+. At a 2:1 excess of Na^+, less than 5% of all conduction events are caused by Na^+. Only in the total absence of K^+ ions, more substantive Na^+ current is seen, which is however much smaller than that in pure K^+ solutions. Error bars depict standard error of the mean (SEM, see also Supplementary Table 1). **(c)** Representative traces of ions traversing the SF of KcsA. The positions in the SF of K^+ ions (purple) and Na^+ ions (yellow) are shown versus simulated time. During periods in which Na^+ binds to the SF, the overall permeation rate is slowed down drastically, whereas in the absence of Na^+ highly efficient K^+ permeation takes place. Representative instantaneous SF occupancies are shown for K^+ permeation (purple circles) and Na^+ permeation (yellow circles), respectively. K^+ and Na^+ ions are displayed as purple and yellow spheres. The permeating K^+ ion is marked in darker colour, and water molecules are shown as red and white spheres.

Fig. 2: The relationship between conduction efficiency, ion selectivity and water co-permeation. (a) The selective channels KcsA, MthK, NaK2K and Kv1.2 W362Y contain four, while the non-selective NaK2CNG-N possesses three SF ion binding sites. **(b)** Currents and water-ion flux ratios at voltages of 220–280 mV in pure and mixed K^+/Na^+ solutions (Error bars: SEM). KcsA, MthK, NaK2K and Kv1.2 W362Y show high K^+ currents in all solutions, lowered by the presence of Na^+ in a concentration-dependent manner (sodium block). MthK, NaK2K and Kv1.2 W362Y strictly exclude Na^+ permeation, with the exception of NaK2K in pure Na^+ solution. The water-ion flux ratio is minimal in all selective channels. Conversely, NaK2CNG-N displays a high level of water permeation in all solutions (water-ion flux ratio >> 1). Water molecules in the SF lead to reduced K^+ currents. **(c)** Simulation snapshots showing outward K^+ permeation events, Na^+ block and relief of Na^+ block in MthK (K^+ ions in purple shades, with the permeating ion darkest, and Na^+ in yellow sphere representation; water molecules in red and white). Here, Na^+ does not reach S4 and is instead replaced by K^+. **(d)** Simulation snapshots of K^+ and Na^+ permeation in NaK2CNG-N (purple and yellow circles, respectively). Direct ion-ion contacts form transiently, but permeation in NaK2CNG-N occurs with intervening water molecules. Periods where only one ion is present in the SF lead to higher water permeation levels. Na^+ ions cross the channel partially hydrated, allowing more water molecules to enter the SF. Control simulations show the robustness of these observations for a wide range of force-field parameters (Supplementary Figs. 1-2). Simulation snapshots for NaK2K and Kv1.2 W362Y are displayed in Supplementary Fig. 3.

Fig. 3: Calculated 2D IR spectrum for occupancy states characteristic for the direct Coulomb knock-on conduction mechanism. Weights used to generate the spectrum are given above the schematic representation of each occupancy. The spectrum displays two pairs of peaks at (ω_{pump}, ω_{probe}) = (1600 cm^{-1}, 1603 cm^{-1}) and (ω_{pump}, ω_{probe}) = (1579 cm^{-1}, 1584 cm^{-1}). These peaks are in good agreement with the experimentally reported values, (ω_{pump}, ω_{probe}) = (1603 cm^{-1}, 1610 cm^{-1}) and (ω_{pump}, ω_{probe}) = (1580 cm^{-1}, 1584 cm^{-1}), when notably only states with direct ion-ion pairs in the SF are taken into account. The spectrum is a linear combination of the spectra of individual states that are frequently visited under permeation conditions (Supplementary Fig. 5). The weights were derived following a protocol from Kratochvil et al[30].

Fig. 4: Schematic representation of the mechanisms of K^+ ion selective (left) and non-selective (right) channel permeation. In selective K^+ channels containing four SF binding sites, ions are observed to permeate largely without their solvation shell (blue). In contrast, we find that non-selective permeation in channels with three SF ion binding sites is based on partial retention of the hydration shell around the ions. The desolvation penalty associated with dehydration of Na^+ ions prevents most Na^+ ions from SF entry (centre, (1)) in the K^+ selective channels. Na^+ ions that surmount this barrier in K^+ selective channels tend to adopt positions between the K^+ binding sites, adding to their ion selectivity (centre, (2)) by impeding efficiently permeating (direct knock-on) conditions.

TABLES

Comparison of IR spectra

Spectrum	Center ω_{pump} (cm^{-1})	Center ω_{probe} (cm^{-1})	Slope	Intensity ratio
Experimental*	1603	1610	0.58 (0.01)	1.25
	1580	1584	0.60 (0.11)	
soft knock-on*	1603	1607	0.51 (0.03)	1.25
	1580	1586	0.52 (0.09)	
soft knock-on	**1609**	**1612**	**0.58 (0.10)**	**1.27**
	1570	**1575**	**0.60 (0.10)**	
direct knock-on	**1600**	**1603**	**0.64 (0.10)**	**1.33**
	1579	**1584**	**0.49 (0.10)**	

Table 1. Properties of experimental and calculated 2D IR spectra. Asterisks (*) indicate data reported in Kratochvil et al., *Science* 2016[30].

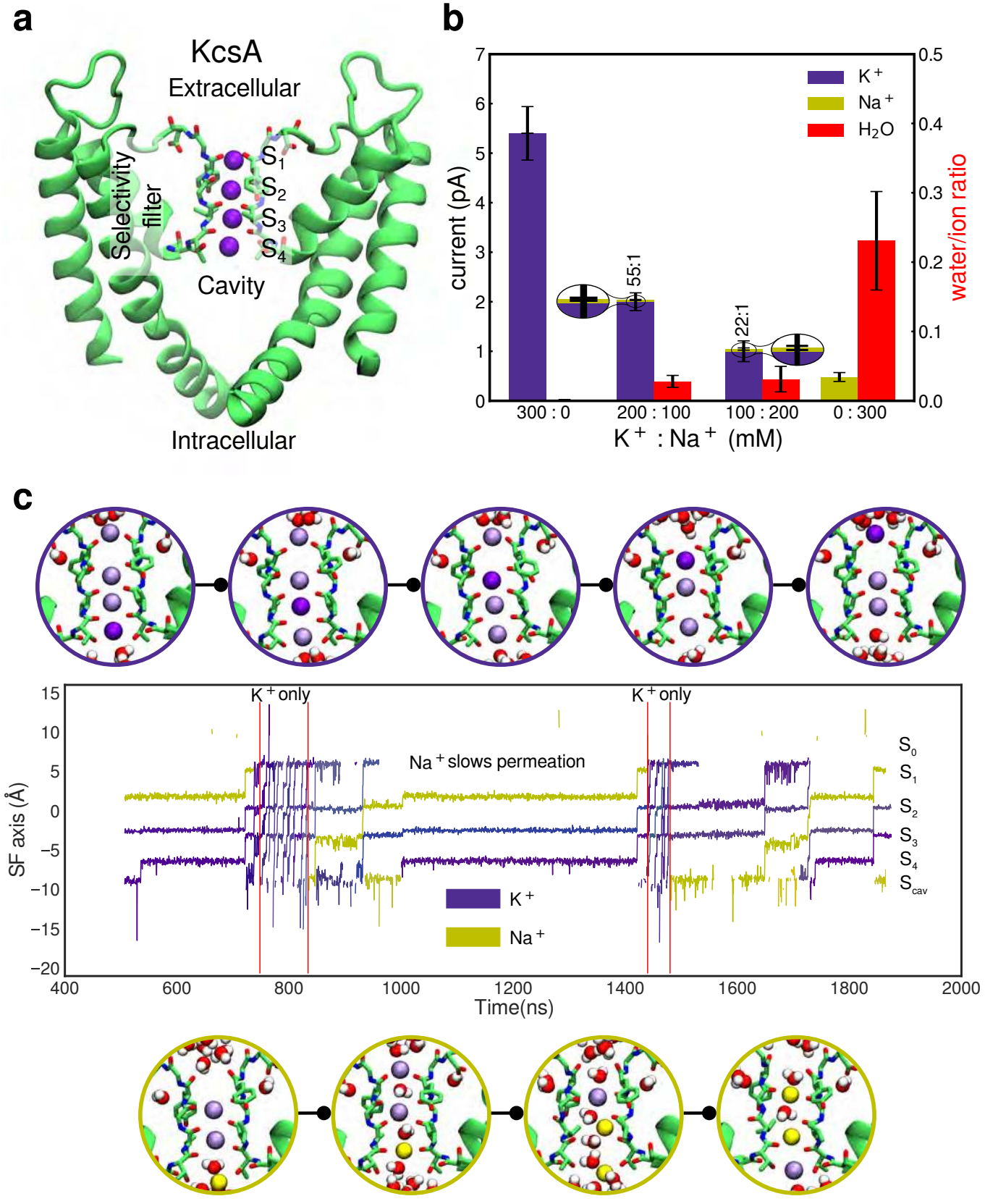
a
KcsA
Extracellular
Selectivity filter
S1
S2
S3
S4
Cavity
Intracellular
b
current (pA)
water/ion ratio
K+
Na+
H2O
55:1
22:1
300 : 0
200 : 100
100 : 200
0 : 300
K+ : Na+ (mM)
c
K+ only
K+ only
Na+ slows permeation
S0
S1
S2
S3
S4
Scav
K+
Na+
SF axis (Å)
Time(ns)

a

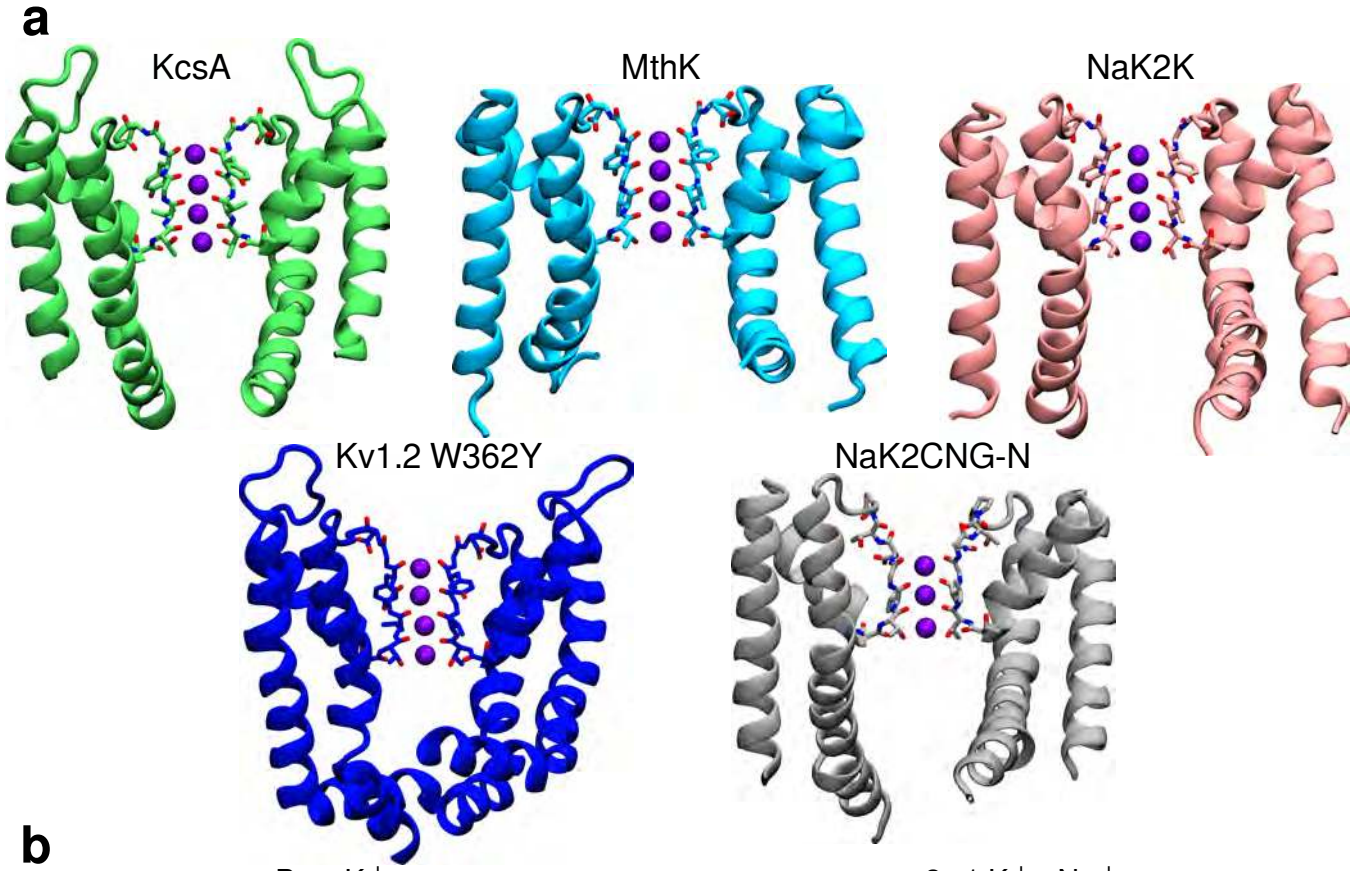
KcsA
MthK
NaK2K
Kv1.2 W362Y
NaK2CNG-N

b

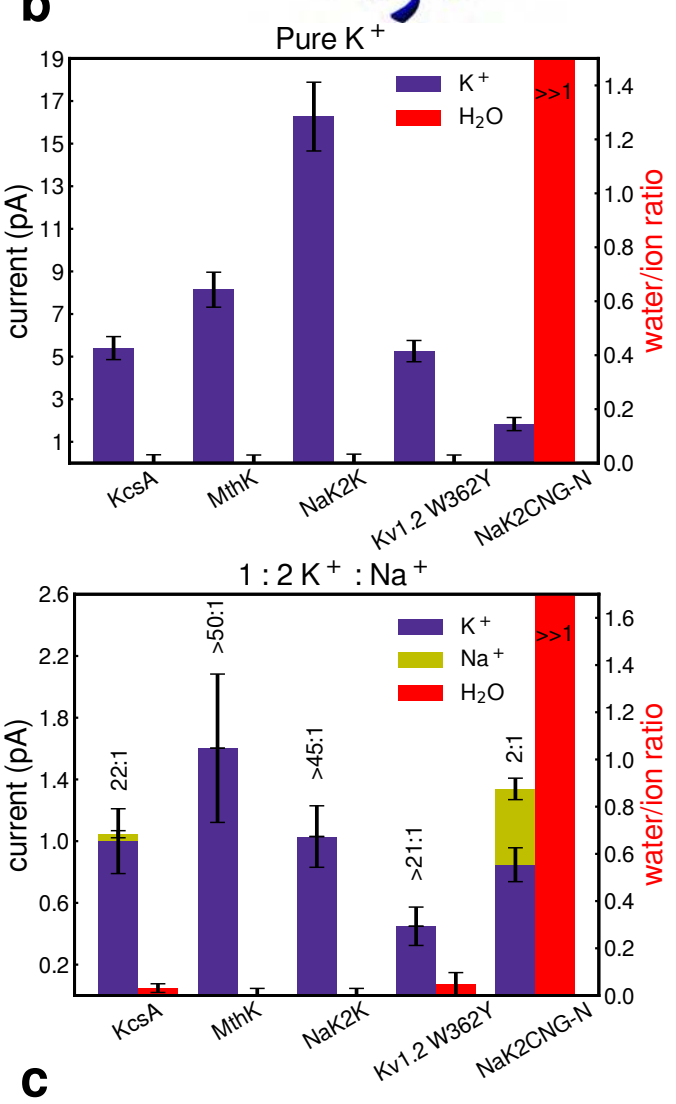
Pure K +
current (pA)
water/ion ratio
K +
H2O
>>1
KcsA
MthK
NaK2K
Kv1.2 W362Y
NaK2CNG-N

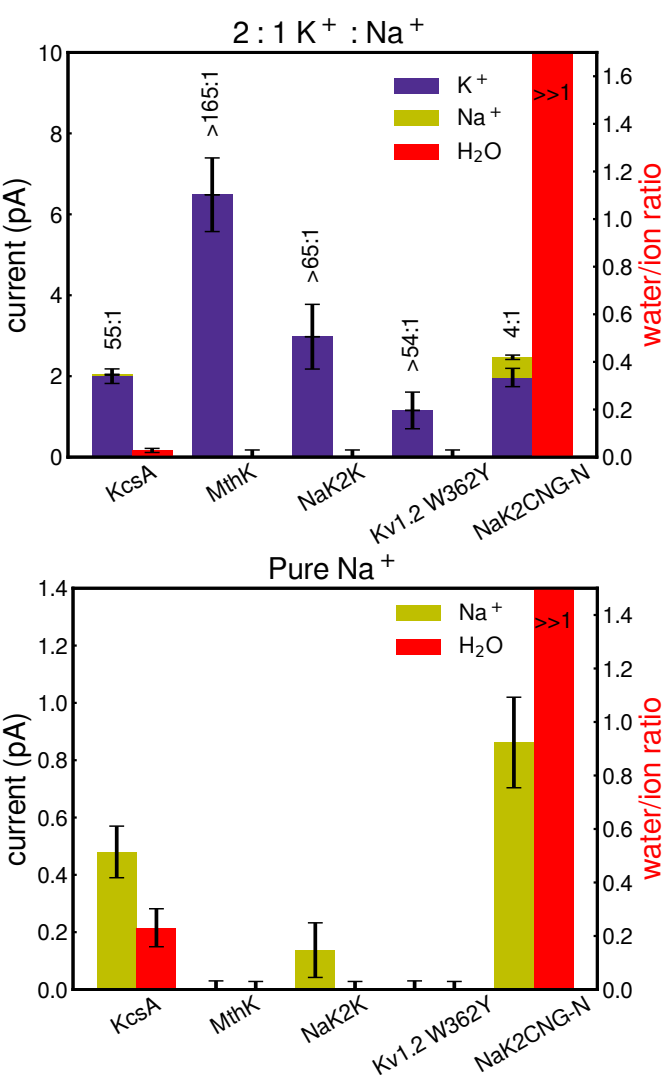
2 : 1 K + : Na +
current (pA)
water/ion ratio
K +
Na +
H2O
55:1
>165:1
>65:1
>54:1
4:1
>>1
KcsA
MthK
NaK2K
Kv1.2 W362Y
NaK2CNG-N

1 : 2 K + : Na +
current (pA)
water/ion ratio
K +
Na +
H2O
22:1
>50:1
>45:1
>21:1
2:1
>>1
KcsA
MthK
NaK2K
Kv1.2 W362Y
NaK2CNG-N

Pure Na +
current (pA)
water/ion ratio
Na +
H2O
>>1
KcsA
MthK
NaK2K
Kv1.2 W362Y
NaK2CNG-N

c

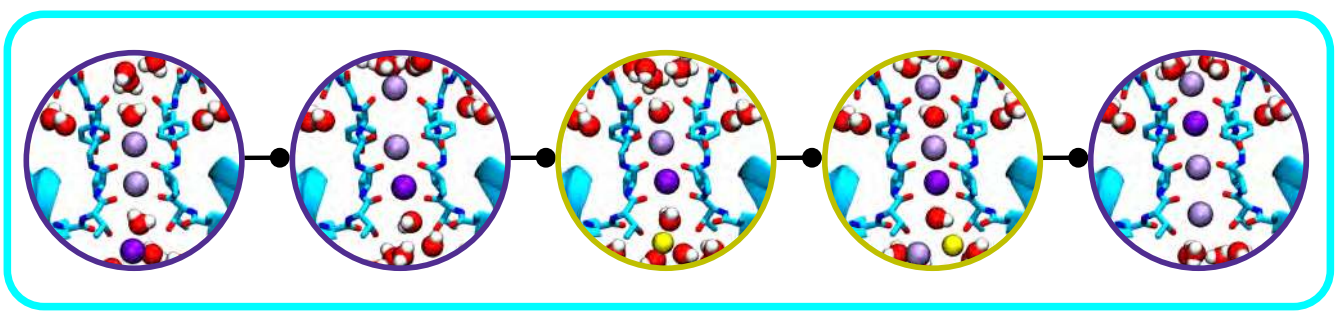

d

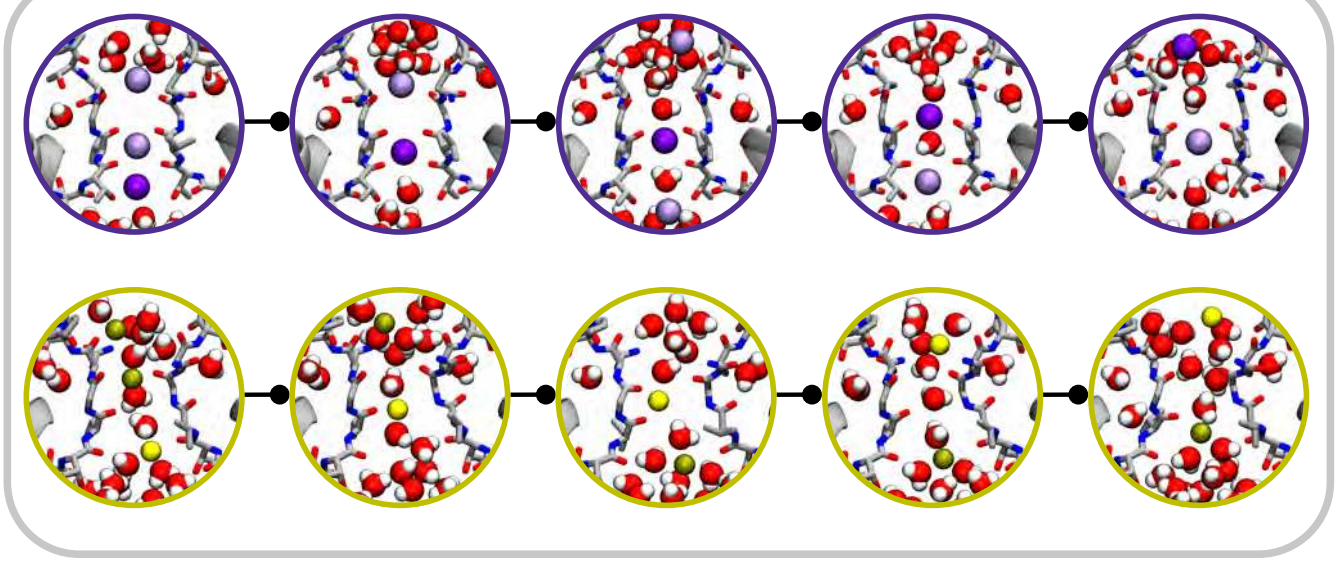

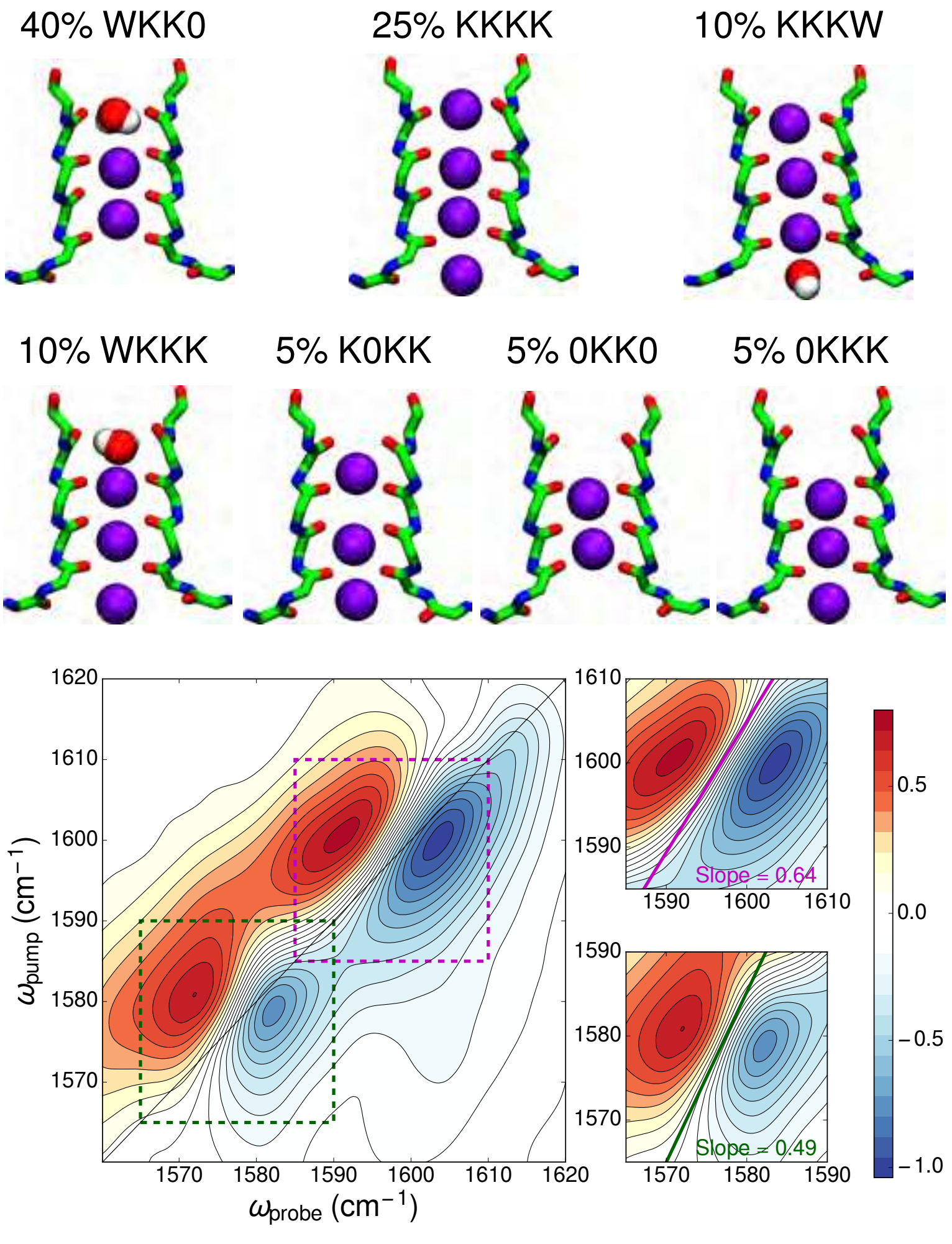
40% WKK0
25% KKKK
10% KKKW
10% WKKK
5% K0KK
5% 0KK0
5% 0KKK
1620
1610
1600
1590
1580
1570
ω_{pump} (cm^{-1})
1570
1580
1590
1600
1610
1620
ω_{probe} (cm^{-1})
Slope = 0.64
Slope = 0.49
0.5
0.0
−0.5
−1.0

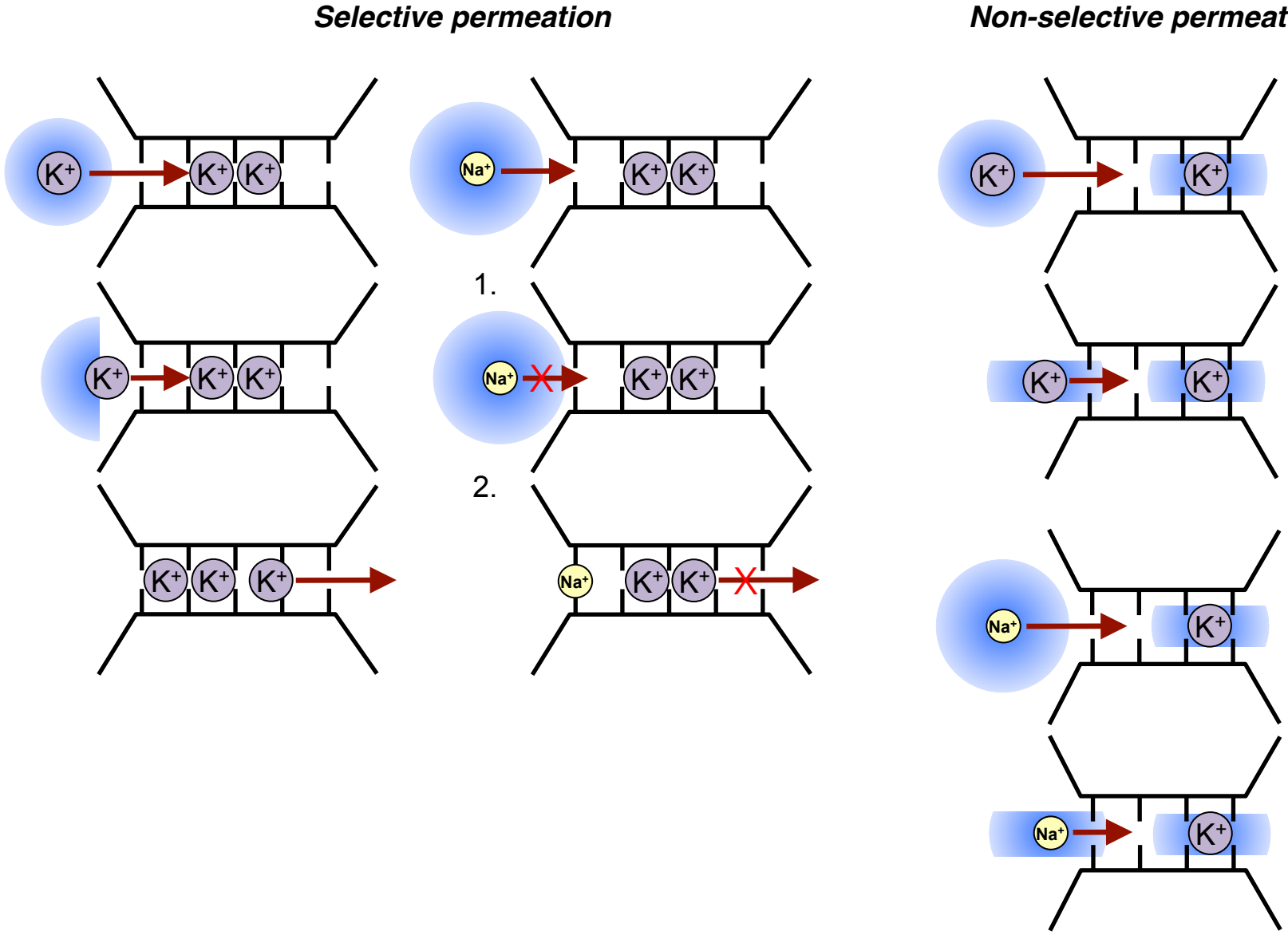
Selective permeation
Non-selective permeation
K+
Na+
1.
2.